forum acusticum 2026
8-12 September · Graz, Austria

SYSTEMATIC PERFORMANCE ANALYSIS OF KT AND HTLS METHODS FOR WAVENUMBER EXTRACTION IN LINED FLOW DUCTS

Anita Schulz[1], Liqun Song[2], Chenyang Weng[3], Zhaohuan Wang[2]

[1] *Faculty 1, University of Applied Sciences Berlin (HTW Berlin), Germany*
[2] *College of Sciences, China Jiliang University, Hangzhou, China*
[3] *Zenseact AB, Gothenburg, Sweden*

This paper is a revised version of the authors' submitted manuscript that was peer-reviewed by at least two anonymous reviewers.

Abstract

The extraction of modal wavenumbers is a fundamental prerequisite for the analysis of complex sound fields in ducts and direct liner impedance eduction. This paper presents a systematic benchmark comparison of the Kumaresan–Tufts (KT) and Hankel total least squares (HTLS) methods for controlled two-dimensional synthetic test cases in lined ducts. First, the methods are tested for single-mode content subject to variations in SNR, noise modeling, and microphone array geometry. Next, a multimodal stress test of a lined duct is conducted, applying impedance boundary conditions for two distinct SDOF Helmholtz resonators. In noise-free cases, both methods recover the reference wavenumbers with near-perfect accuracy. Under noisy conditions, the extraction error increases by roughly one decade per 20 dB reduction in SNR. Furthermore, turbulent boundary-layer noise is slightly more detrimental than white noise at low SNRs. HTLS proves to be globally more robust, particularly for modes with a positive imaginary part. Regarding array design, KT and HTLS perform comparably for favorable $k_x h$ values in the fourth quadrant, with limits and optima dictated by Δx and l. While the current parametric investigation is not exhaustive, it confirms the expected dominance of the dimensionless products $k_x \Delta x$ and $k_x l$. These initial insights serve as a starting point for future systematization efforts.

Keywords: *mode decomposition, wavenumber extraction, impedance eduction, face-to-face measurements*

Corresponding author: *anita.schulz@htw-berlin.de.*

1. Introduction

Direct impedance eduction based on face-to-face microphone measurements is attractive because it does not require an *a priori* assumption of the acoustic field and, in principle, allows the liner impedance to be inferred directly from the measured modal content [1], [2]. In practice, however, the quality of the final impedance estimate depends critically on the preceding extraction of the complex axial wavenumbers k_x. This intermediate step is often treated as a black box, although it can introduce substantial uncertainty, especially in multimodal sound fields and in the presence of flow noise. Among the available modal decomposition methods, the Kumaresan–Tufts (KT) algorithm [3] is one of the most established approaches in duct acoustics [1], [4], [5], [6], while Hankel total least squares (HTLS) [7] represents a closely related subspace-based alternative that has only recently been introduced into impedance eduction [8]. Existing uncertainty studies mainly address the educed impedance itself [5], [8], whereas a systematic assessment of the k_x-extraction performance is still lacking. The present paper addresses this gap by evaluating KT and HTLS through controlled synthetic benchmark cases for lined ducts. To this end, the influence of modal wavenumber, modal order, microphone array geometry, and measurement noise is systematically investigated. The analysis progresses from single-mode reference cases to a multimodal stress test based on SDOF liner impedances.

2. Methodological Setup

All benchmark cases considered here are based on an infinitely long two-dimensional channel of constant height h, and axial wavenumbers are reported in the dimensionless form $k_x h$.

2.1. Compared Methods

The Kumaresan–Tufts (KT) algorithm and the Hankel total least squares (HTLS) are two established high-resolution methods for axial wavenumber extraction of acoustic modes in ducts. Only a brief summary is given here, since KT has already been described in more detail in the context of impedance eduction in previous work [1], [4], while HTLS was introduced for this application more recently by Yang et al. [8]. KT is a Prony-type backward linear-prediction method, whereas HTLS is a closely related subspace-based variant. Both methods estimate damped complex exponentials from multichannel pressure data. In theory, HTLS is expected to be more robust than KT once noise and model errors become important. The reason is that KT is based on a linear-prediction formulation, whereas HTLS uses a total-least-squares subspace treatment of the Hankel data matrix and therefore accounts for perturbations on both sides of the underlying regression problem. In consequence, HTLS is expected to be less sensitive to bias from noisy data matrices, correlated disturbances, and mild model mismatch. At the same time, this advantage need not be large in the favorable single-mode case with correct model order, where both methods estimate the same isolated pole from well-structured data. In all benchmarks, the extraction order was prescribed from the known synthetic setup; no adaptive MDL-based rank selection or separate parameter study was performed here.

2.2. Error Metric

The performance of the wavenumber extraction is measured by the L_2 distance between the extracted and reference axial wavenumber. For the single-mode case considered first, this reduces to

$$e_{\mathrm{L}_2} = |k_{x,\mathrm{est}} - k_{x,\mathrm{true}}|. \tag{1}$$

Unless stated otherwise, the results present Monte Carlo mean errors obtained over 200 noise realizations. An absolute error metric was preferred because it remains well conditioned over the full investigated complex-wavenumber range, whereas relative normalization becomes fragile when the reference magnitude is small.

2.3. Noise Models

To simulate realistic measurement conditions, synthetic noise is added to the spatially sampled pressure signals across the virtual microphone array. Two noise models are considered. The first is spatially uncorrelated complex Gaussian white noise, which serves as the baseline case. The second is a turbulent boundary layer (TBL) noise model with a Goody wall-pressure spectrum [9] and a Corcos-type spatial coherence model [10]. For a prescribed signal-to-noise ratio (SNR), the added noise power is scaled consistently between both models, so that the comparison isolates the effect of spatial correlation and spectral structure rather than a change in overall noise level.

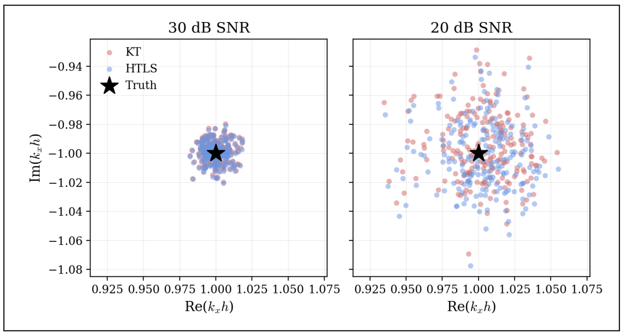

Figure 1: Monte Carlo estimates of the KT and HTLS methods for a single injected mode in the complex $k_x h$ plane under Gaussian white noise at SNR = 30 dB and 20 dB (200 realizations). The black star denotes the true value.

For the TBL model, $\delta = 0.5h$, the wall shear stress was estimated from a hydraulic Reynolds number via a Blasius-type friction law, the Corcos parameters were fixed to $U_c/U = 0.6$ and $\alpha = 0.12$, and SNR was defined from the ratio of mean signal power to mean noise power over all microphones and frequencies.

3. Single-Mode Injection Study

The systematic evaluation starts with the most controlled case, namely single-mode injection. Only one mode is present in the synthesized pressure field, and the extraction methods are informed that exactly one mode is to be identified. This removes ambiguities related to mode matching and model-order overestimation and isolates the intrinsic estimator sensitivity.

3.1. Influence of the Signal-to-Noise Ratio

As a first representative illustration, Fig. 1 shows Monte Carlo clouds for the representative wavenumber $k_x h = 1 - i$ under Gaussian white noise at 30 dB (left) and 20 dB (right). As expected, both methods produce nearly symmetric scatter around the true value, and the spread increases as the SNR decreases. The corresponding mean L_2 errors are 9.33×10^{-3} (KT) and 9.26×10^{-3} (HTLS) at 30 dB, and 2.95×10^{-2} (KT) and 2.96×10^{-2} (HTLS) at 20 dB.

The results for a systematic variation of the SNR are shown in Fig. 2 for injected modes with $k_x h = n(1-i)$, $n = 1, 3, 5, 9$. The mean error increases by approximately one decade for each 20 dB decrease in SNR. This behavior is consistent with the expectation that, in the moderate-noise regime, the wavenumber estimate can be linearized around the noise-free solution, such that the extraction error scales approximately with the noise amplitude rather than with the noise power. The same figure also shows that the sensitivity increases with modal wavenumber magnitude and that HTLS remains slightly more robust for larger n.

Figs. 3 and 4 give an overview of the extraction error in the complex wavenumber plane. For both white noise and TBL noise, the dominant variation is associated with the imaginary part of k_x, whereas the dependence on $\Re(k_x)$ remains comparatively weak. This stripe-like structure stems from the pole representation $z = \exp(-ik_x \Delta x)$. In this formulation,

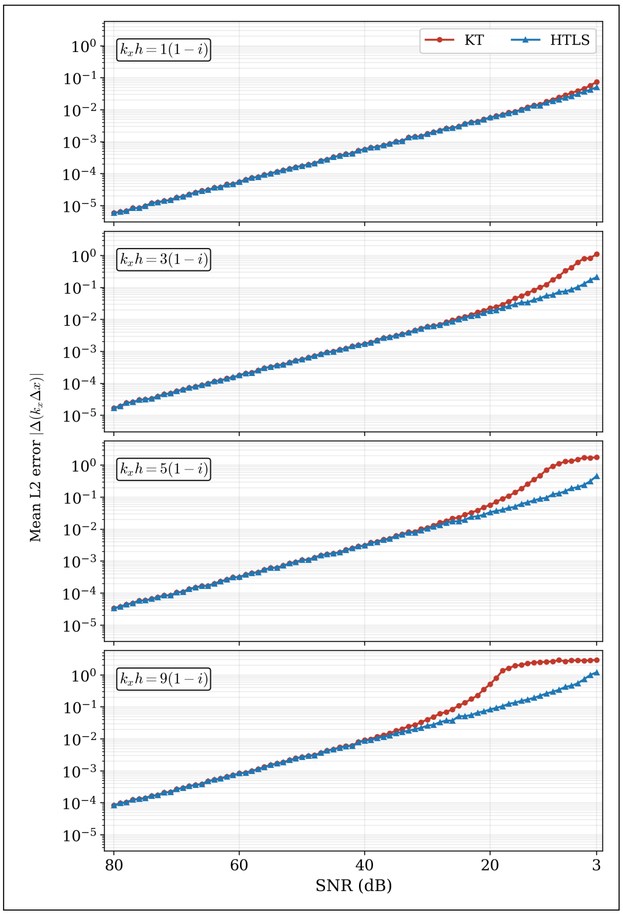

Figure 2: Mean L_2 extraction error versus SNR for injected modes with $k_x h = n(1 - i)$, $n = 1, 3, 5, 9$, under Gaussian white noise. The curves compare the KT and HTLS methods based on 200 Monte Carlo realizations per case.

$\Re(k_x)$ determines the phase angle of the pole, whereas $\Im(k_x)$ dictates its magnitude. Consequently, $\Im(k_x)$ controls the spatial growth or decay across the array, thereby directly governing both the effective SNR and the numerical conditioning of the estimation problem.

A clear difference between the two methods appears for modes with positive imaginary part. In this region, KT performs poorly even at high nominal SNR, because exponentially growing waves combined with the backward-prediction structure of KT lead to an ill-conditioned estimation problem. HTLS is less affected and therefore remains more robust. The TBL case is not uniformly worse than Gaussian white noise, but it becomes clearly more detrimental at lower SNR, where the correlated turbulent fluctuations become more difficult to distinguish from the physical modal content.

3.2. Influence of Microphone Spacing and Number

The microphone array geometry – specifically the spacing Δx and the number of equidistant sensors m – was varied for injected modes $k_x h = n(1 - i)$ with $n = 1, \ldots, 5$. All configurations were subjected to TBL noise at a fixed SNR $= 40$ dB. The

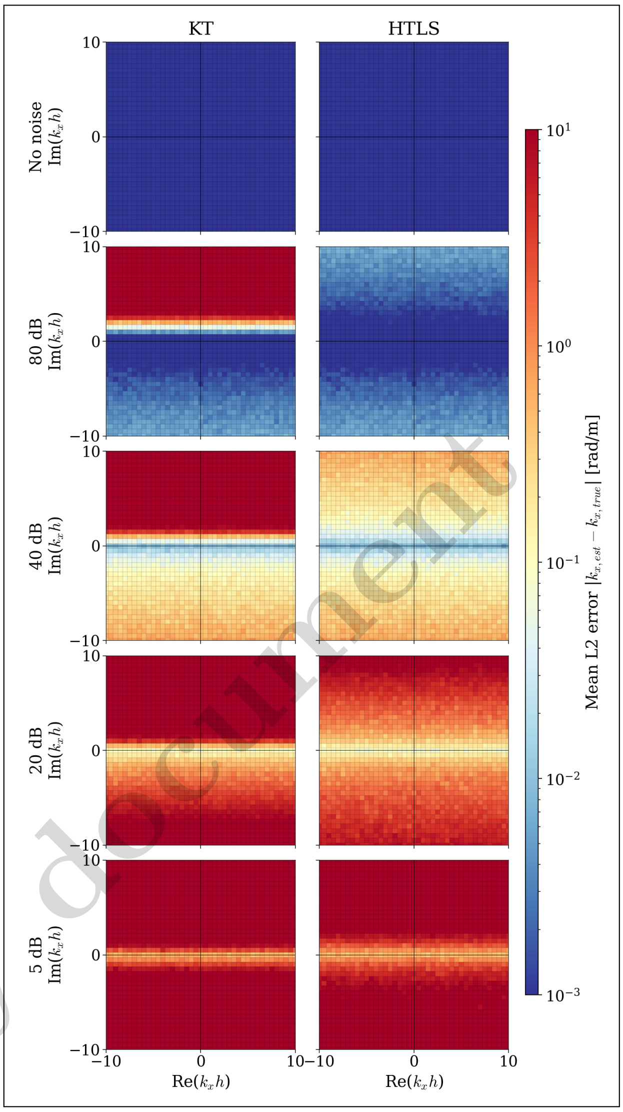

Figure 3: L_2 error of KT (left) and HTLS (right) based wavenumber extractions in the complex $k_x h$ plane for spatially uncorrelated Gaussian white noise. Rows indicate decreasing SNR values from top to bottom.

tested parameter space included dimensional spacings of $\Delta x = 4, 8, 12, 16, 20, 24$ mm and array sizes of $m = 8, 12, 16, 24, 32, 40, 56, 80$. Across the heatmaps and representative sweeps in Figs. 5 to 7, the governing dimensionless quantities are $k_x \Delta x$ and $k_x l$, where $l = (m - 1)\Delta x$ denotes the total array length. Physically, $k_x \Delta x$ dictates the local phase shift between adjacent microphones, whereas $k_x l$ describes the total phase progression across the entire array, which determines its overall spatial resolution.

The clearest trend relates to the microphone number m (see e.g. Fig. 6 for a representative HTLS result; KT behaves similarly). Increasing m extends the array length and thus increases $k_x l$, which reduces the extraction error by capturing more spatial information. The improvement then saturates once $k_x l$ is sufficiently large.

The dependence on Δx is non-monotonic, as illustrated in the HTLS results in Fig. 7; KT shows the same trend. Since Δx enters through $z =$

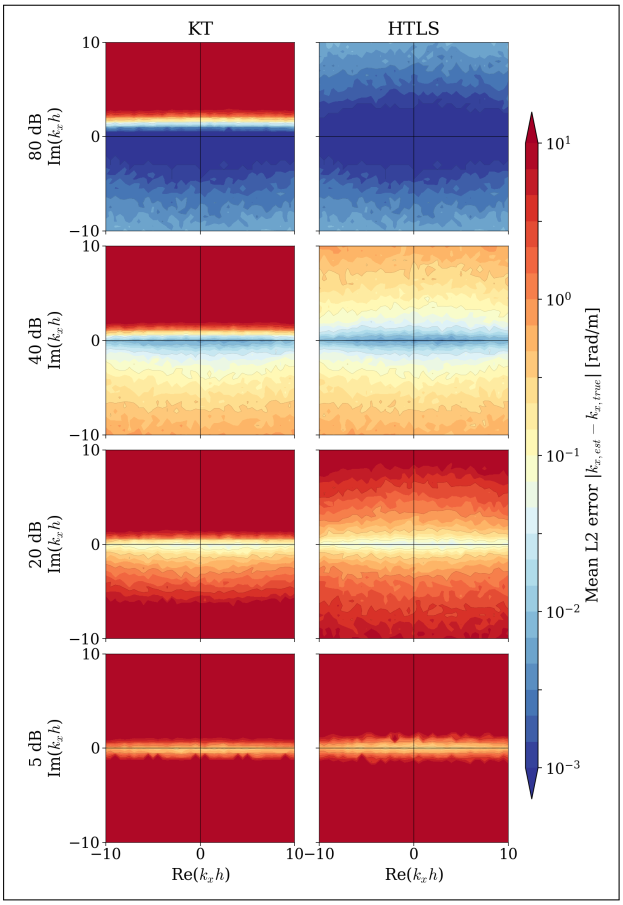

Figure 4: Same as Fig. 3, but for turbulent boundary layer (TBL) noise.

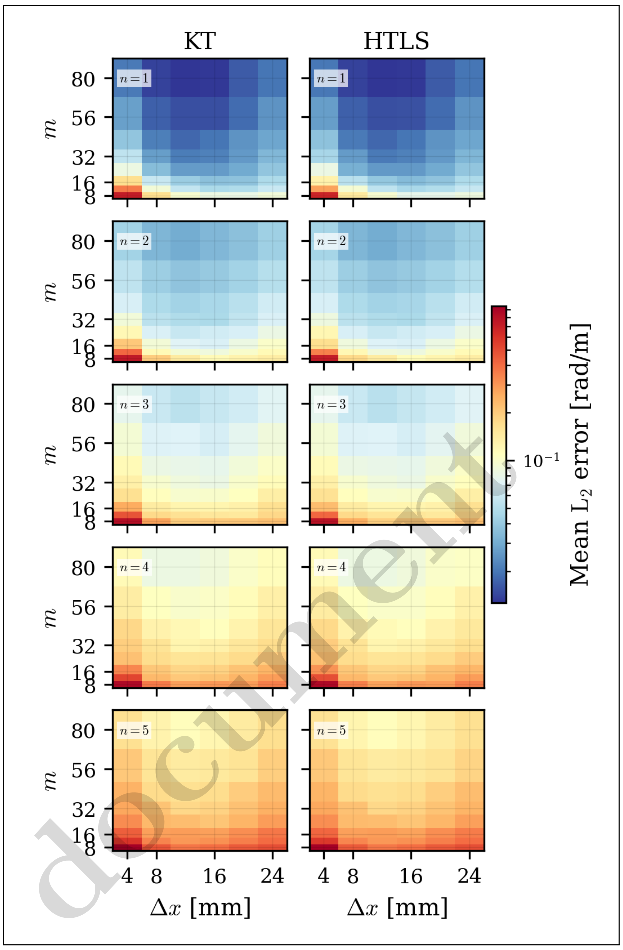

Figure 5: Mean L_2 extraction error in the $(\Delta x, m)$ plane for $k_x h = n(1-i)$, $n = 1, \ldots, 5$, at SNR = 40 dB with TBL noise. Rows denote the injected modes $n = 1, \ldots, 5$, columns denote KT and HTLS methods.

$\exp(-ik_x\Delta x)$, very small spacings yield only weak local phase differences, whereas very large spacings lead to poor spatial sampling and phase ambiguity. The error therefore exhibits a broad optimum at intermediate spacings. The trends of KT and HTLS remain remarkably similar throughout the single-mode geometry study. This is expected, as both methods estimate the same damped exponential pole from identical single-mode data using the correct model order. Under these favorable conditions, the dominant limitation is therefore not the specific estimator structure, but rather the geometric conditioning of the inverse problem itself. More pronounced differences between KT and HTLS are anticipated primarily when the problem becomes more severely ill-conditioned, for example in the presence of multiple nearby poles, stronger correlated disturbances, or more extreme modal growth and decay. For this reason, Fig. 8 presents the collapse map – plotting $\Re(k_x l)$ against $\Re(k_x\Delta x)$ – only for the HTLS results, as the corresponding KT representation exhibits the exact same trend. In this plot, the results from all individual parameter variations align along orderly lines. This consistent alignment proves that the dimensionless products $k_x l$ and $\Re(k_x\Delta x)$ are indeed the systematic governing quantities, rather than the absolute geometric parameters alone. These trends are specific to the present infinite-duct benchmark and should not be transferred directly to finite lined-duct configurations, where reflections and lined-to-rigid transitions may alter the geometry dependence. As shown in Fig. 8, the error peaks near the right margin ($\Re(k_x\Delta x) \approx 1.5$ rad with small l), where coarse spatial sampling and phase ambiguity degrade estimation. Conversely, prominent error minima (dark regions) emerge when moderate local phase increments are paired with sufficiently large array lengths, ensuring well-conditioned matrices. In the present diagonal test family ($k_x h = n(1-i)$), the wavenumbers lie on a diagonal line passing through the second and fourth quadrants of the complex plane. Consequently, the real and imaginary parts of k_x are proportionally coupled rather than varied independently, so that projecting the data solely onto $\Re(k_x\Delta x)$ and $\Re(k_x l)$ already provides a compact and faithful representation of the trend. A more general design map would instead need to retain the full complex dependence of k_x. This data collapse suggests that optimal microphone spacings and array lengths might indeed be identified from admissible regions within this dimensionless space. At the same time, this should still be regarded as a preliminary indication rather than a complete design rule, since the corresponding analysis has not yet been extended to other directions in the complex

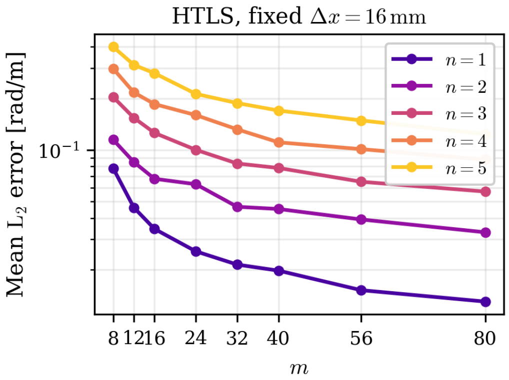

Figure 6: Mean L_2 extraction error versus microphone number m for HTLS at fixed $\Delta x = 16\,\mathrm{mm}$, $\mathrm{SNR} = 40\,\mathrm{dB}$, and TBL noise. The curves correspond to injected modes $k_x h = n(1-i)$, $n = 1, \ldots, 5$.

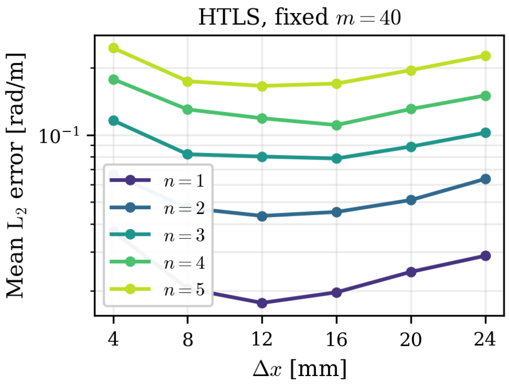

Figure 7: Mean L_2 extraction error versus microphone spacing Δx for HTLS at fixed $m = 40$, $\mathrm{SNR} = 40\,\mathrm{dB}$, and TBL noise. The curves correspond to injected modes $k_x h = n(1-i)$, $n = 1, \ldots, 5$.

k_x plane or to a broader range of noise conditions.

4. Multimodal Study

To move closer to practical applications, the analysis is extended to a multimodal scenario based on two no-flow SDOF Helmholtz-resonator liners from Schulz et al. [11]: a medium-resistance case ($\Re(Z)/(\rho c) \approx 0.5$, resonance at $\approx 850\,\mathrm{Hz}$) and a low-resistance case ($\Re(Z)/(\rho c) \approx 0.15$, resonance at $\approx 1230\,\mathrm{Hz}$). Their reference wavenumbers were computed over 200 to 2200 Hz. The total pressure field was synthesized from the two least attenuated right-running modes, and both KT and HTLS were given the exact true extraction order of two. TBL noise was added at a fixed $\mathrm{SNR} = 20\,\mathrm{dB}$, roughly representative of the natural level around Mach 0.4 in the present setup. Two arrays were compared: a reference case with $\Delta x = 16\,\mathrm{mm}$ and $m = 40$, and a sparse case with $\Delta x = 32\,\mathrm{mm}$ and $m = 10$.

The error maps in Fig. 9 show that the low-resistance liner spans a much larger region of the complex $k_x h$ plane and is therefore harder to decompose. For both liners, the sparse array yields larger errors than the reference geometry, consistent with the reduced phase information discussed previously. KT and HTLS ex-

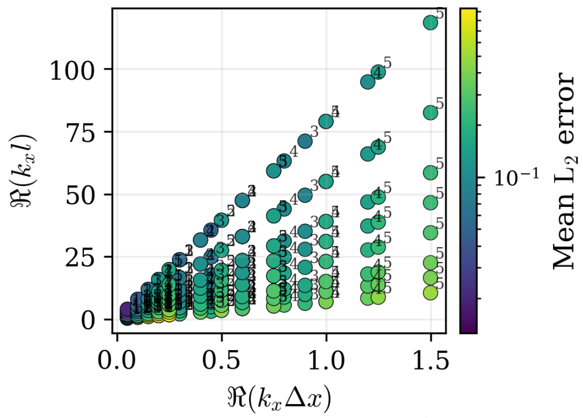

Figure 8: Preliminary collapse of the diagonal geometry study onto the dimensionless groups $\Re(k_x \Delta x)$ and $\Re(k_x l)$ (HTLS, $\mathrm{SNR} = 40\,\mathrm{dB}$, TBL noise).

hibit the same qualitative trends, but HTLS remains slightly more robust in several regions. Overall, realistic multimodal sound fields constitute a markedly more severe stress test than idealized single-mode benchmarks.

5. Conclusions and Outlook

Main findings of the present study can be summarized as follows:

- In noise-free synthetic benchmark cases, KT and HTLS both recover the damped-exponential signal model essentially exactly.
- Under noisy conditions, HTLS is globally more robust and is particularly superior for modes with positive imaginary part, where KT can fail because of the unfavorable conditioning of the backward-prediction formulation.
- For the single-mode benchmark, the error depends approximately linearly on the logarithmic scale, corresponding to roughly one decade increase in extraction error for each 20 dB reduction in SNR.
- Turbulent boundary-layer noise is more critical than white noise mainly at lower SNR, but the difference remains moderate compared with the overall SNR effect.
- For practically relevant fourth-quadrant cases, KT and HTLS show similar geometric dependencies governed by the dimensionless products $k_x \Delta x$ and $k_x l$. While an increased array length improves extraction via $k_x l$, the local spacing Δx exhibits a broad intermediate optimum. Note that this geometric mapping is preliminary and does not yet cover the full complex k_x plane.
- The multimodal example confirms that realistic sound fields are significantly more demanding to decompose than idealized single-mode benchmarks.

The present work serves as a foundational step. Next steps include unknown multimodal sound fields, axial flow variations, higher-dimensional effects, and application to experimental data. A particularly relevant

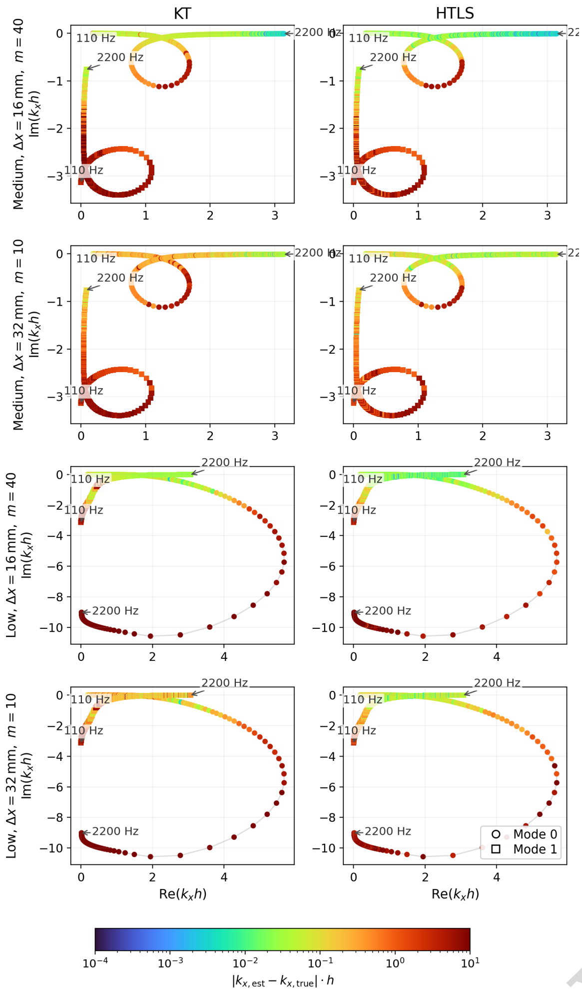

Figure 9: Wavenumber extraction error in the complex $k_x h$ plane for the multimodal benchmark with medium- and low-resistance SDOF liners, reference and sparse array geometries, and TBL noise at SNR = 20 dB. Columns show the KT and HTLS results.

next step is the extension to finite lined ducts, for example with mode-matching approaches, to capture reflections and lined-to-rigid transition effects more realistically; algorithmic choices such as rank truncation and pencil parameters should also be included in future sensitivity studies. More robust, data-driven decomposition strategies should also be explored. The long-term goal is practical guidance for engineers who need to infer the modal content of lined ducts when the contributing modes are not known in advance.

Conflict of interest

The authors state that they have no conflicts of interest to disclose. Regarding author Chenyang Weng, this research was conducted independently on his own time and is unrelated to his employment at Zenseact AB. No company resources or proprietary information from Zenseact AB were used in this work.

References

[1] W. R. Watson, M. H. Carpenter, and M. G. Jones, "Performance of kumaresan and tufts algorithm in liner impedance edution with flow," *AIAA Journal*, vol. 53, no. 4, pp. 1091–1102, 2015.

[2] C. Weng, A. Schulz, D. Ronneberger, L. Enghardt, and F. Bake, "Flow and viscous effects on impedance eduction," *AIAA Journal*, vol. 56, no. 3, pp. 1118–1132, 2018.

[3] R. Kumaresan and D. W. Tufts, "Estimating the parameters of exponentially damped sinusoids and pole-zero modeling in noise," *IEEE Transactions on Acoustics, Speech, and Signal Processing*, vol. 30, no. 6, pp. 833–840, 1982.

[4] C. Weng, A. Schulz, D. Ronneberger, L. Enghardt, and F. Bake, "Impedance eduction in the presence of turbulent shear flow using the linearized navier-stokes equations," in *Proc. of the 23rd AIAA/CEAS Aeroacoustics Conference*, 2017.

[5] L. A. Bonomo, A. M. N. Spillere, and J. A. Cordioli, "Parametric uncertainty analysis for impedance eduction based on prony's method," *AIAA Journal*, vol. 58, no. 8, p. 15, 2020.

[6] R. Roncen, E. Piot, F. Méry, F. Simon, M. G. Jones, and D. M. Nark, "Wavenumber-based impedance eduction with a shear grazing flow," *AIAA Journal*, vol. 58, no. 7, 2020.

[7] J.-M. Papy, L. D. Lathauwer, and S. V. Huffel, "Common pole estimation in multi-channel exponential data modeling," *Signal Processing*, vol. 86, no. 4, pp. 846–858, 2006.

[8] J. Yang, T. Humbert, J. Golliard, and G. Gabard, "Direct impedance eduction of acoustic liners in multimodal ducts with shear flows," *Journal of Sound and Vibration*, vol. 626, p. 119 635, 2026.

[9] M. Goody, "Empirical spectral model of surface pressure fluctuations," *AIAA Journal*, vol. 42, no. 9, pp. 1788–1794, 2004. DOI: 10.2514/1.9433

[10] G. M. Corcos, "The structure of the turbulent pressure field in boundary-layer flows," *Journal of Fluid Mechanics*, vol. 18, no. 3, pp. 353–378, 1964. DOI: 10.1017/S002211206400026X

[11] A. Schulz, F. Bake, L. Enghardt, and D. Ronneberger, "Impedance eduction of acoustic liners based on four different levels of physical modeling," in *Proc. of the 22th AIAA/CEAS Aeroacoustics Conference*, 2016.